

# An Innovative Phyto-mediated Nanocomposite-modified Glass Ionomer Cement: A Detailed Study on Synthesis, Cytotoxicity, Anti-inflammatory Effects, Antimicrobial Activity, Mechanical Performance, and Solubility

Aleena Alex<sup>1</sup>, Jessy Paulraj<sup>2</sup>, Subhabrata Maiti<sup>3</sup>, Rajeshkumar Shanmugam<sup>4</sup>

Received on: 25 August 2024; Accepted on: 12 October 2024; Published on: 20 March 2025

## ABSTRACT

**Background:** Glass ionomer cement (GIC), or polyalkenoate cement, is popular for esthetic restorations due to its tooth-bonding ability but suffers from low mechanical strength, abrasion resistance, and moisture sensitivity, leading to the search for better alternatives.

**Aim:** To evaluate the cytotoxicity, anti-inflammatory, antimicrobial, mechanical properties, and solubility of phyto-mediated nanocomposite-modified GIC.

**Materials and methods:** Chitosan-titanium-zirconia-hydroxyapatite (Ch-Ti-Zr-HA) nanocomposites were synthesized using a single-step phyto-mediated process and added to GIC at 3, 5, and 10% concentrations (groups I, II, and III), with conventional GIC as the control (group IV). Characterization was done, and the effects on cytotoxicity, anti-inflammatory response, antimicrobial activity, compressive strength, flexural strength, microhardness, and solubility were assessed and analyzed using one-way analysis of variance (ANOVA) and the Tukey *post hoc* test.

**Results:** Characterization confirmed all particles were within the nanoscale. A 10 wt% concentration of phyto-mediated Ch-Ti-Zr-HA nanocomposite enhanced antimicrobial activity against *Streptococcus mutans* and *Lactobacillus*. It also improved compressive strength ( $197.29 \pm 0.253$  MPa), flexural strength ( $34.71 \pm 0.223$  MPa), and microhardness ( $50.35 \pm 0.232$  MPa) compared to conventional GIC ( $p \leq 0.05$ ). Solubility was lowest at 10% ( $0.053 \pm 0.005$ ), followed by 5% ( $0.056 \pm 0.005$ ), 3% ( $0.086 \pm 0.005$ ), and conventional GIC ( $0.113 \pm 0.005$ ), with significance ( $p < 0.05$ ). Toxicological analysis showed no significant toxicity, and anti-inflammatory properties were stable. The modified GIC with phyto-mediated nanocomposite shows potential as a dental restorative material, especially in regions of high stress.

**Conclusion:** Our findings indicate that 10% phyto-mediated Ch-Ti-Zr-HA nanocomposite-modified GIC excels in antibacterial activity, compressive and flexural strength, microhardness, and solubility, outperforming conventional GIC and showing potential for enhanced dental applications.

**Keywords:** Modified-glass ionomer cement, Nanomaterials, Phytomedicine, Restorative dentistry.

*International Journal of Clinical Pediatric Dentistry* (2025); 10.5005/jp-journals-10005-3071

## INTRODUCTION

Glass ionomer cement (GIC) is widely used in dentistry for its anticaries properties, biocompatibility, and strong dentin bonding.<sup>1</sup> Tooth-colored materials like conventional GIC and composite resins are preferred, but composite resins are challenging for pediatric and special needs patients due to isolation and moisture control issues.<sup>2</sup> GIC faces issues such as initial dehydration and high swelling rates, which compromise its mechanical and antibacterial properties, leading to reports of caries recurrence after restoration.<sup>3</sup> Recurrent carious lesions are often localized, making alternatives like crowns impractical in some cases. Incomplete sealing of restorations allows cariogenic bacteria to persist, leading to caries recurrence and restoration failure.<sup>4</sup> Hence, improving restorative materials to ensure strong seals and enhanced antimicrobial properties is crucial. Therefore, combining antibacterial agents with GIC could offer a promising solution.

Dental restorative cements are exposed to tooth tissue and physiological fluids, so they must be biocompatible throughout their use. Cytotoxicity testing assesses the biocompatibility of these

<sup>1,2</sup>Department of Pediatric and Preventive Dentistry, Saveetha Dental College and Hospitals, Saveetha Institute of Medical and Technical Sciences, Saveetha University, Chennai, Tamil Nadu, India

<sup>3</sup>Department of Prosthodontics, Saveetha Dental College and Hospitals, Saveetha Institute of Medical and Technical Sciences, Saveetha University, Chennai, Tamil Nadu, India

<sup>4</sup>Department of Pharmacology, Saveetha Dental College and Hospitals, Saveetha Institute of Medical and Technical Sciences, Saveetha University, Chennai, Tamil Nadu, India

**Corresponding Author:** Jessy Paulraj, Department of Pediatric and Preventive Dentistry, Saveetha Dental College and Hospitals, Saveetha Institute of Medical and Technical Sciences, Saveetha University, Chennai, Tamil Nadu, India, Phone: +91 8861646189, e-mail: drjessy2019@gmail.com

**How to cite this article:** Alex A, Paulraj J, Maiti S, *et al.* An Innovative Phyto-mediated Nanocomposite-modified Glass Ionomer Cement: A Detailed Study on Synthesis, Cytotoxicity, Anti-inflammatory Effects, Antimicrobial Activity, Mechanical Performance, and Solubility. *Int J Clin Pediatr Dent* 2025;18(2):181–190.

materials, particularly when placed in deep cavities where there is a risk of indirect contact with pulp cells.<sup>5</sup> Additionally, masticatory and parafunctional forces can cause deformation of restorations. Thus, a material's clinical effectiveness depends on its ability to endure masticatory stresses and strains. Strength is crucial for preventing deformation and fractures, thereby reducing the risk of restoration failure.

Plants have long been used for medicinal purposes, a practice that continued until the development of chemistry in the 16th century. Phytomedicine, which uses plant extracts and components, is considered minimally toxic.<sup>6</sup> Recently, nanotechnology has advanced dental restorations by incorporating nanosized fillers such as silver, zinc, titanium dioxide, zirconia, silica, and graphene, enhancing their mechanical properties.<sup>7</sup> Thus, the green-mediated nanoparticles were synthesized to form a nanocomposite in order to reduce potential hazards. Nanoflakes or nanoparticles like titanium dioxide and hydroxyapatite have proven to be excellent nanoscale fillers. Their inclusion in dental materials has significantly strengthened dental substrates.<sup>8</sup>

In the past decade, nanoscale hydroxyapatite<sup>9</sup> and HA-silica ( $\text{SiO}_2$ )<sup>10</sup> have been successfully used to enhance GICs. More recently, nanosized zirconia ( $\text{ZrO}_2$ ) and HA- $\text{ZrO}_2$  combinations<sup>11</sup> have been explored to further strengthen GIC. Zirconium oxide, recognized for its excellent dimensional stability and durability comparable to stainless steel, has been used to reinforce brittle HA bio-glasses in biomedical applications.<sup>12</sup> A recent study on HA- $\text{SiO}_2$ - $\text{ZrO}_2$  enhanced GICs showed promising results for microhardness.<sup>13</sup> However, there is limited information on their compressive and flexural strengths, and potential toxicity to pulp cells from these nanoparticles needs further investigation.

This study aimed to evaluate a novel phyto-mediated chitosan (Ch), titanium (Ti), zirconia (Zr), and hydroxyapatite (HA) nanocomposite-modified GIC, testing the hypothesis that it does not improve antibacterial and physicochemical properties.

## MATERIALS AND METHODS

### Study Design and Sample Size Assessment

Ethical approval was granted, and the *in vitro* study was officially registered under code SRB/SDC/UG-1889/23/PEDO/069. Sample size was calculated using G\*Power, which indicated that 48 samples were required for most parameters at 0.95 power and 0.6 effect size.

### Synthesis of Phyto-mediated Nanoparticles

**Synthesis of phyto-mediated chitosan nanoparticles:** One gm of dried eucalyptus leaves was boiled in 100 mL distilled water, heated to 60–80°C for 5–10 minutes, then cooled and filtered. 0.5 gm chitosan was mixed with 0.5 gm acetic acid and 49 mL distilled water, stirred until clear, and 4–5 drops of sodium tripolyphosphate were added. The eucalyptus extract and chitosan solution were mixed, stirred on a magnetic stirrer, and incubated at 37°C.

**Synthesis of phyto-mediated titanium oxide nanoparticles:** Glassware was sterilized and dried. About 1 gm neem leaves was boiled in 100 mL water for 5–10 minutes and filtered. 0.365 gm titanium oxide was dissolved in 50 mL distilled water, then mixed with neem extract, stirred, and incubated at 37°C.

**Synthesis of phyto-mediated zirconium oxide nanoparticles:** One gm aloe vera powder was boiled in 100 mL water at 40–50°C for 5–10 minutes, cooled, and filtered. About 20 millimolar

**Source of support:** Nil

**Conflict of interest:** None

zirconium oxychloride octahydrate was mixed with 50 mL distilled water. Aloe vera extract was mixed with the zirconium solution, stirred at 340–360 RPM, and stored overnight on an orbital shaker.

**Synthesis of phyto-mediated hydroxyapatite nanoparticles:** Eggshells were cleaned, boiled at 80°C for 30 minutes, dried at 80°C for 24 hours, and heated at 1000°C for 2 hours. The eggshells were ground into CaO powder. 1 gm moringa oleifera leaves was boiled in 100 mL distilled water. About 0.1 gm of CaO was combined with 50 mL distilled water and mixed with 50 mL moringa extract. The mixture was stirred for 2 hours, orthophosphoric acid was added (Ca/P ratio 1.67), stirred for 30 minutes, and stored for 24 hours to undergo aging.

### Fabrication of Phyto-mediated Nanocomposites

The nanocomposites were developed using a one-pot approach.<sup>14</sup> Solutions of chitosan, titanium oxide, zirconium oxide, and hydroxyapatite nanoparticles were mixed and stirred at 80°C for 30 minutes. Then, 1.08 mL of ethanol was added, and the mixture was stirred at 80°C under reflux for 90 minutes. Ethanol was evaporated at 80°C for 30 minutes, and the solution was freeze-dried at –92°C for 48 hours to yield a fine powder that can enhance nanoparticle stability and preserve their properties.

### Fabrication of Phyto-mediated Nanocomposite Modified Glass Ionomer Cement

NanoCh-Ti-Zr-HA powder was added to conventional GIC at 3, 5, and 10% by weight as group I, group II, and group III. The Ch-Ti-Zr-HA nanocomposite powder and GIC powders were weighed and manually ground for 10 minutes using a pestle and mortar. The mixtures were then combined with type IX GIC liquid, transferred to molds for compression, and cured at 37°C and 100% relative humidity for 24 hours (Fig. 1). Conventional GIC type IX served as the control. After characterization, the samples were tested for physicochemical properties.

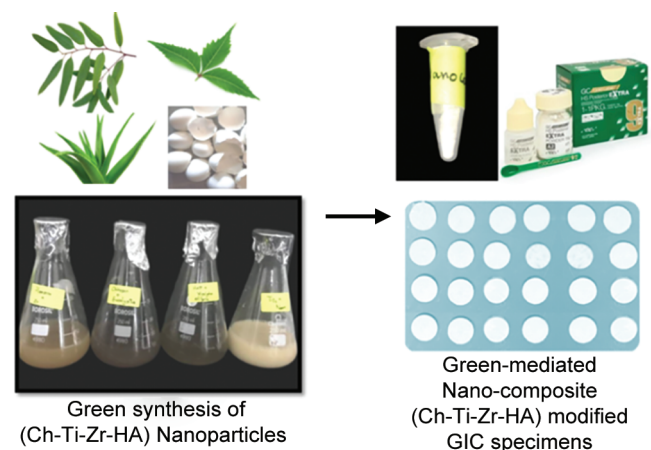


**Fig. 1:** Phyto-mediated synthesis of Ch-Ti-Zr-HA nanocomposite-modified GIC



## Characterization of Phyto-mediated Nanocomposite Modified Glass Ionomer Cement

Fourier transform infrared spectroscopy (FTIR): FTIR analysis of the GIC nanoCh-Ti-Zr-HA powder was recorded using a Nicolet iS10 (Thermo Fisher Scientific) within the 500–3500  $\text{cm}^{-1}$  range. The instrument's standard spectral resolution of 4  $\text{cm}^{-1}$  was employed to examine the chemical bonds in the samples.

Scanning electron microscopy (SEM): The structural characteristics of the nanoCh-Ti-Zr-HA GIC powder were examined with a Jeol JSM IT-800 SEM (Germany). Samples were gold-coated using a Desk-II sputter coater (Denton Vacuum Inc., NJ, USA) at approximately 50 mTorr and 40 mA.

Energy dispersive X-ray (EDX): The chemical composition of the nanoCh-Ti-Zr-HA modified GIC was semiquantitatively analyzed using an EDX analyzer (FEA-USA (S.E.A.) PTE LTD).

## Cytotoxicity Testing

Brine Shrimp Lethality Assay: About 2 gm of iodine-free salt was dissolved in 200 mL distilled water. Six-well enzyme-linked immunosorbent assay (ELISA) plates were filled with 10–12 mL of saline in each well, and 10 nauplii were added to each. Different volumes of the nanocomposite-modified GIC samples (20, 40, 60, 80, and 100) were added based on the concentration levels. The plates were left to incubate for 24 hours, after which the number of live nauplii was observed and recorded.

## Anti-inflammatory Testing

Bovine serum albumin (BSA) denaturation assay: The anti-inflammatory activity of the Ch-Ti-Zr-HA modified GIC was tested using the BSA denaturation assay. BSA (0.45 mL) was mixed with the nanocomposite (10–50 ng/mL) at pH 6.3, incubated at room temperature for 10 minutes, and at 55°C for 30 minutes. Diclofenac sodium was the standard, and dimethyl sulfoxide served as the control. Denaturation was measured at 660 nm.

## Antimicrobial Testing

Specimen preparation: Type IX GIC (GC Corporation) was used in this study, with phyto-mediated nanocomposite (Ch-Ti-Zr-HA) added at 3, 5, and 10% concentrations. The polyacrylic acid-based liquid (GC Corporation) was mixed to form a uniform paste. The mixture was placed into 5 mm diameter and 2 mm thick molds using a sterile cement carrier and leveled with a sterile glass slide. After setting, the samples were inspected under bright light for porosities or cracks, with any defective specimens excluded. All samples were finished, polished, and stored at room temperature.

Time kill curve assay: A time-kill curve assay was conducted to assess the bactericidal effect and concentration-dependent activity of phyto-mediated nanocomposite Ch-Ti-Zr-HA modified GIC against *Streptococcus mutans* and *Lactobacillus*. Pathogens were cultured in Mueller Hinton Broth with 3, 5, and 10% nanocomposite-modified GIC, and time-kill curves were analyzed. Following a 5-hour preincubation without antimicrobial agents, growth curves were established to confirm pathogens were in the early-to-mid log phase. A 0.5 McFarland inoculum was made from cultures grown on Mueller Hinton agar plates at 37°C for 18–20 hours, then diluted in prewarmed Mueller Hinton Broth, and 90  $\mu\text{L}$  of this mixture was added to each well of a 96-well ELISA plate. About 10  $\mu\text{L}$  of nanocomposite-modified GIC at different concentrations was added to each well, along with an untreated control. The plates were incubated under suitable conditions for 1–5 hours. The dead cell

percentage was determined by measuring absorbance at 540 nm using an ELISA reader.

## Compressive Strength

Cylindrical samples (4 × 6 mm) were formed using stainless-steel split molds following ISO 9917-1: 2007. A thin layer of cocoa butter was applied to the molds to facilitate sample removal. The material was placed in the molds, and the samples were covered with polyester strips and glass slides, then gently pressed to remove trapped air. After 30 minutes, the molds were carefully removed, and the samples were stored in distilled water at 37°C for 24 hours. After conditioning, each sample was tested using a universal testing machine (Instron Electro Plus® E3000), with a compressive load applied along the longitudinal axis at 1 mm/minute until failure, and compressive strength was measured in megapascals (MPa).

## Flexural Strength

Beam-shaped samples (3 × 3 × 25 mm) were made in stainless-steel molds per ISO 9917-2: 2007, then kept at 37°C and 100% humidity for 50 minutes, followed by immersion in distilled water at 37°C for 23 hours. The samples were tested using a three-point bending test in an Instron E3000 at 0.5 mm/minute and a 20 mm span, or 50 ± 16 N/minute, with flexural strength recorded.

## Microhardness

In Vickers microhardness testing, a diamond pyramid is pressed onto the surface under a set load for a specified duration. The Shimadzu HMV-G31DT tester used a 2.942 N load (HV0.3) for 20 seconds, and the hardness number is calculated based on the indentation width.

## Solubility

Samples were formed in a stainless-steel mold with a 5 mm diameter and 2 mm thickness. Each material was mixed as per instructions, the mold was placed on a glass slab and covered with a polyester strip, and pressed with a glass slide until set. Defective samples were discarded. After 1 hour, samples were stored in a desiccator for 2 hours, and the samples were then kept at 37°C for 22 hours to reach a constant mass ( $\pm 0.0005$  gm). Initial weights were recorded. Samples were then immersed in 25 mL deionized water in labeled bottles and incubated at  $37 \pm 1^\circ\text{C}$  for 7 days. After incubation, samples were dried with cotton, dehydrated at  $37 \pm 1^\circ\text{C}$  for 24 hours, and reweighed. Solubility was determined from the mass difference.

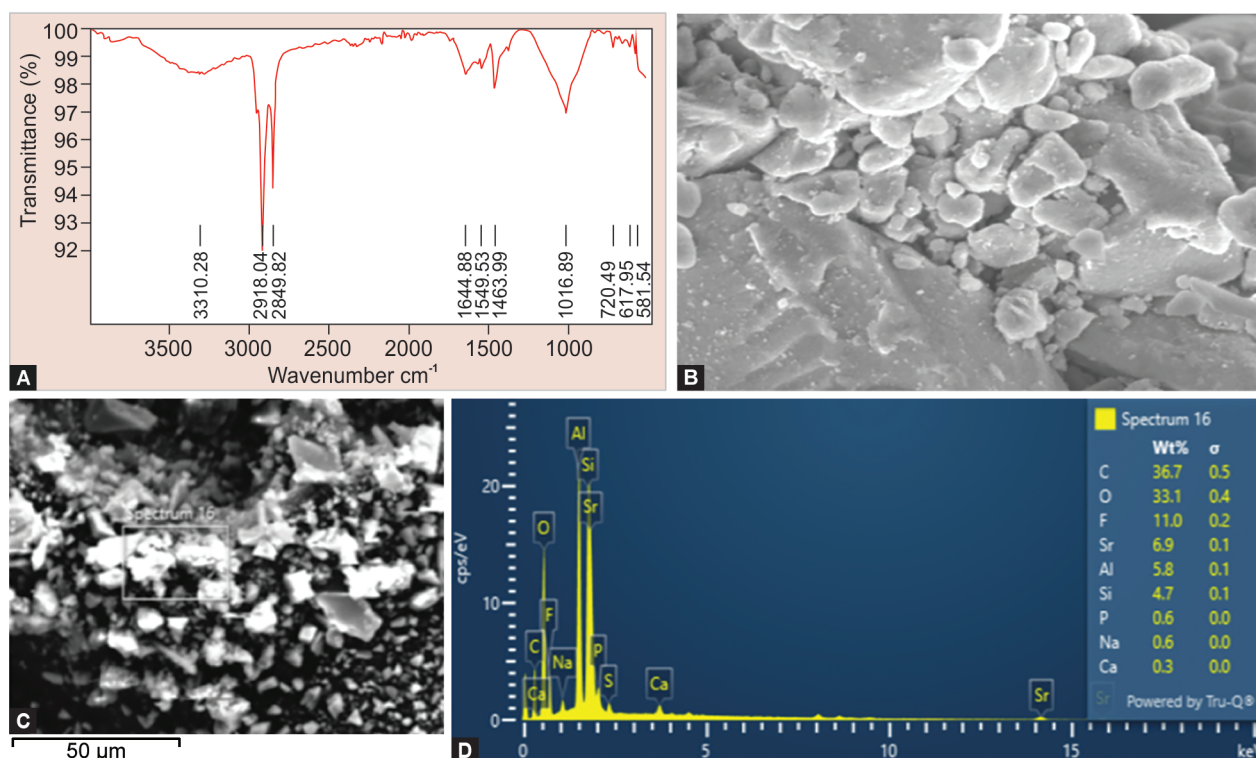
## Statistical Analysis

Data analysis was done using SPSS version 23.0, with numerical data presented as mean  $\pm$  SD, assuming normal distribution. Statistical significance was set at  $p \leq 0.05$ . One-way analysis of variance (ANOVA) was used to evaluate overall differences, and Tukey's honestly significant difference (HSD) *post hoc* test identified specific group differences. A significance level of  $p < 0.05$  was used.

# RESULTS

## Characterization Interpretations

FTIR analysis of the nanocomposite Ch-Ti-Zr-HA nanocomposite GIC was recorded using a Nicolet iS10 spectrometer (Thermo Fisher Scientific) over the range of 500–3500  $\text{cm}^{-1}$ . The instrument's



**Figs 2A to D:** Characterization of phyto-mediated nanocomposite-modified GIC: (A) FTIR pattern; (B) SEM micrograph under 33,000 $\times$  magnification; (C) EDX spectral analysis; (D) EDX elemental analysis

resolution was between 0.16 and 0.5  $\text{cm}^{-1}$ . Variations in absorption peaks were observed (Fig. 2A). The peak at 3310.28  $\text{cm}^{-1}$  corresponded to OH stretching vibrations from absorbed water. Peaks at 2918.04  $\text{cm}^{-1}$  and 2849.82  $\text{cm}^{-1}$  indicated OH vibrations. The band at 1644.88  $\text{cm}^{-1}$  was attributed to the carboxyl group stretching, confirming  $\nu_3$  stretching of  $\text{PO}_4^{3-}$ . Peaks at 1549.53  $\text{cm}^{-1}$  and 1463.99  $\text{cm}^{-1}$  (related to  $\text{PO}_4^{3-}$  bending and Ti–O, Zr–O stretching) were replaced by a broad peak at 1016.28  $\text{cm}^{-1}$  in the GIC. A small peak at 720.49  $\text{cm}^{-1}$  in the nanoCh-Ti-Zr-HA spectra shifted to 617.95  $\text{cm}^{-1}$ , likely due to  $\text{CaF}_2$  or  $\text{Al}_2\text{O}_3$ . A new peak at 581.54  $\text{cm}^{-1}$  indicated bending vibrations of  $\text{AlPO}_4$  and  $\text{Al}_2\text{O}_3$ . These results suggest molecular interactions between nanoCh-Ti-Zr-HA and GIC, confirming the successful integration of the nanocomposites into the GIC matrix.

SEM analysis of GIC after nano modification at various concentrations shows clear changes in surface morphology. With increasing nano filler concentration, the microstructure improves. At lower concentrations, SEM images reveal a granular surface with scattered nanoparticles, indicating minor changes to the GIC matrix. Higher concentrations lead to a denser, more uniform distribution of nanoparticles, resulting in a more uniform and denser structure. The SEM images confirm that nanoCh-Ti and nano  $\text{ZrO}_2$  fill the gaps between HA rods, creating a denser nanoCh-Ti-Zr-HA powder. High magnification (33,000 $\times$ ) shows that nanoHA rods have a rough texture, likely covered by fine  $\text{TiO}_2$  and  $\text{ZrO}_2$  residues (Fig. 2B). Similar observations were noted in other studies.<sup>15</sup> Energy dispersive X-ray analysis identified key elements in the nanoCh-Ti-Zr-HA powder as Ca, P, Al, Na, F, and O, with smaller amounts of Zr, Ch, and Ti (Fig. 2C and D). This confirms the formation of the nanoCh-Ti-Zr-HA nanocomposite and suggests potential improvements in mechanical properties and overall performance.

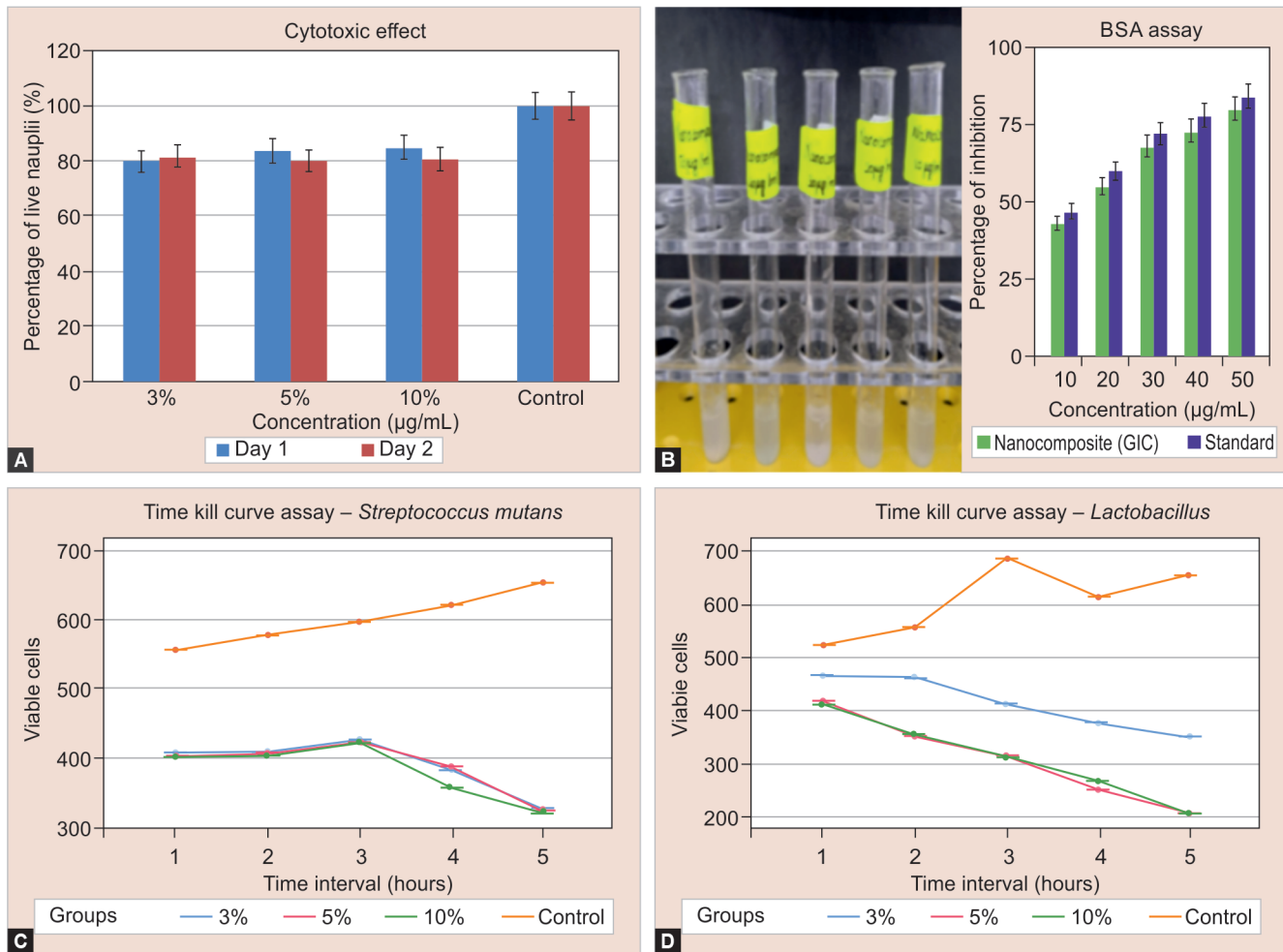
### Evaluation of Cytotoxicity and Anti-inflammatory Effects

The cytotoxicity of the nanocomposite Ch-Ti-Zr-HA modified GIC was assessed using the brine shrimp lethality assay. The results demonstrated a cytotoxic effect that was dependent on concentration. On day 1, the 5  $\mu\text{g}$  concentration had 100% live nauplii, similar to the control group. By day 2, survival rates were lower than the control (Fig. 3A). At 40  $\mu\text{g}$  and 80  $\mu\text{g}$ , nauplii survival stabilized at 50%, indicating a plateau in cytotoxicity with higher concentrations.

The anti-inflammatory effects of the Ch-Ti-Zr-HA nanocomposite were evaluated using the BSA denaturation assay. Inhibition rates ranged from 47% at 10  $\mu\text{g}/\text{mL}$  to 81% at 50  $\mu\text{g}/\text{mL}$ , demonstrating strong anti-inflammatory activity (Fig. 3B). The nanocomposite's effect was comparable to the standard across all concentrations.

### Assessment of Antibacterial Activity

The susceptibility of pathogenic carious organisms, *S. mutans* and *Lactobacillus*, to nanocomposite Ch-Ti-Zr-HA modified GIC was tested. A time-kill kinetics study assessed the antimicrobial activity of this modified GIC at concentrations of 3, 5, and 10%. For *S. mutans*, the modified GIC showed significantly better performance than conventional GIC, especially at the 10% concentration, exhibiting strong antimicrobial effects (Fig. 3C). Tukey's HSD test revealed significant differences between the control and the nanocomposite-modified groups (Table 1). The modified GIC groups consistently showed better antibacterial activity for *Lactobacillus* than the control, with the 10% concentration demonstrating superior performance (Fig. 3D). Pairwise comparisons showed significant differences, with the control group demonstrating the lowest effectiveness



**FIGS 3A to D:** Cytotoxicity, anti-inflammatory, and antimicrobial activity of phyto-mediated nanocomposite-modified GIC: (A) Brine shrimp lethality assay; (B) BSA assay; (C) Antimicrobial efficacy against *S. mutans*; (D) Antimicrobial efficacy against *Lactobacillus*

**Table 1:** Pairwise comparison of antimicrobial efficacy on *S. mutans* between all groups

Groups	Mean difference	Std. error	95% confidence interval		p-value
			Lower bound	Upper bound	
3 vs 5%	0.002	0.0002	0.001	0.002	0.001*
3 vs 10%	0.010	0.0002	0.009	0.010	0.001*
3% vs control	-0.211	0.0002	-0.211	-0.210	0.001*
5 vs 3%	-0.002	0.0002	-0.002	-0.001	0.001*
5 vs 10%	0.008	0.0002	0.007	0.008	0.001*
5% vs control	-0.213	0.0002	-0.214	-0.212	0.001*
10 vs 3%	-0.010	0.0002	-0.010	-0.009	0.001*
10 vs 5%	-0.008	0.0002	-0.008	-0.007	0.001*
10% vs control	-0.221	0.0002	-0.222	-0.221	0.001*

\*Significant at the 0.05 level; the *p*-value was derived from multiple comparisons by Tukey's honestly significant difference; The error term is mean square (error) = 1.500E-7

(Table 2). The nanocomposite Ch-Ti-Zr-HA modified GIC demonstrated a concentration-dependent bactericidal effect, with complete bacterial elimination at higher concentrations. The nanocomposite's distinctive size improved its ability to penetrate bacterial cells, leading to damage and thereby improving bactericidal activity against both *S. mutans* and *Lactobacillus*.

### Assessment of Physicomechanical Properties

One-way ANOVA indicated significant differences in compressive strength, flexural strength, and microhardness ( $p = 0.001$ ) (Table 3). The 10% concentration of nanocomposite-modified GIC exhibited the highest compressive strength ( $197.29 \pm 0.253$ ) (Fig. 4A), flexural strength ( $34.71 \pm 0.223$ ) (Fig. 4B), and microhardness ( $50.35 \pm 0.232$ ) (Fig. 4C), surpassing the 5%, 3%,



**Table 2:** Pairwise comparison of antimicrobial efficacy on *Lactobacillus* between all groups

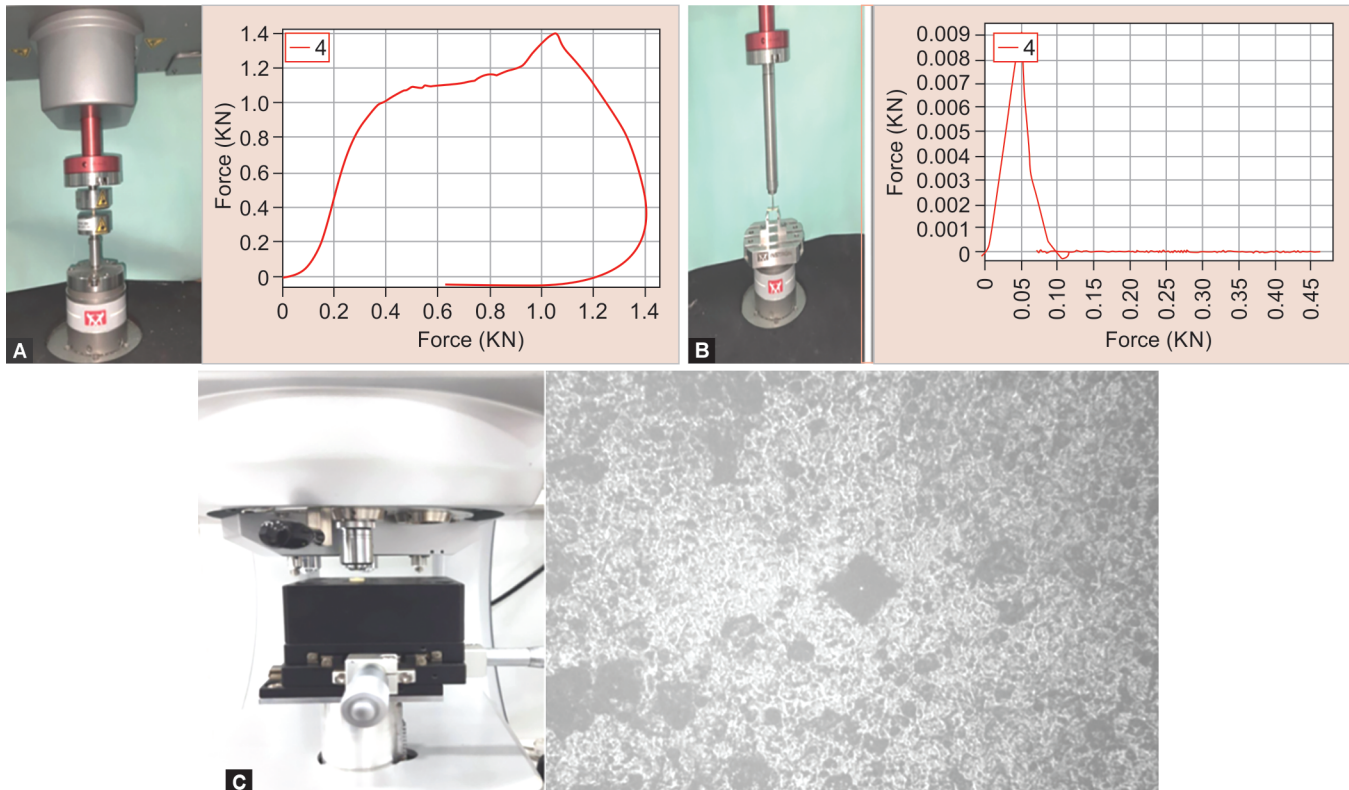
Groups	Mean difference	Std. error	95% confidence interval		p-value
			Lower bound	Upper bound	
3 vs 5%	0.105	0.00026	0.104	0.105	0.001*
3 vs 10%	0.103	0.00026	0.102	0.103	0.001*
3% vs control	-0.193	0.00026	-0.194	-0.192	0.001*
5 vs 10%	-0.002	0.00026	-0.002	-0.001	0.001*
5% vs control	-0.298	0.00026	-0.299	-0.297	0.001*
10% vs control	-0.296	0.00026	-0.297	-0.295	0.001*

\*Significant at the 0.05 level; the *p*-value was derived from multiple comparisons by Tukey's honestly significant difference; The error term is mean square (error) = 2.063E-7

**Table 3:** Comparison of strength and microhardness of phyto-mediated nanocomposite (Ch-Ti-Zr-HA)-modified GIC and conventional GIC

Variables	Groups	N	Mean $\pm$ SD	Std. error	Lower bound	Upper bound	F value	p-value
Compressive	3%	12	178.57 $\pm$ 0.105	0.0304	178.508	178.642	7052.56	0.001*
	5%	12	189.75 $\pm$ 0.052	0.0150	189.716	189.783		
	10%	12	197.29 $\pm$ 0.253	0.0733	197.130	197.453		
	Control	12	167.85 $\pm$ 1.025	0.2960	167.206	168.509		
Flexural	3%	12	27.12 $\pm$ 0.045	0.0130	27.095	27.152	25718.10	0.001*
	5%	12	31.67 $\pm$ 0.247	0.0714	31.513	31.828		
	10%	12	34.71 $\pm$ 0.223	0.0646	34.575	34.859		
	Control	12	16.86 $\pm$ 0.019	0.0055	16.847	16.872		
Microhardness	3%	12	45.44 $\pm$ 0.286	0.0827	45.267	45.631	3939.37	0.001*
	5%	12	48.58 $\pm$ 0.144	0.0417	48.489	48.673		
	10%	12	50.35 $\pm$ 0.232	0.0670	50.205	50.500		
	Control	12	41.65 $\pm$ 0.144	0.0417	41.559	41.743		

\*Statistically significant value of *p* < 0.05. The *p*-value was derived from a one-way ANOVA test



**Figs 4A to C:** Physicomechanical properties of phyto-mediated nanocomposite-modified GIC: (A) Compressive strength analysis; (B) Flexural strength analysis; (C) Microhardness analysis

and control groups. Tukey's HSD pairwise comparison confirmed that the nanocomposite-modified GIC groups were significantly more effective than the control group in all tested properties (Table 4).

### Assessment of Solubility

One-way ANOVA analysis showed significant differences in water solubility across the groups ( $p < 0.05$ ), with an  $F$  value of 148.33 (Table 5). Among all the groups, the 10% concentration exhibited the lowest solubility ( $0.053 \pm 0.005$ ), followed by the 5% ( $0.056 \pm 0.005$ ), 3% ( $0.086 \pm 0.005$ ), and control ( $0.113 \pm 0.005$ ) groups, respectively. Pairwise comparison indicated significant differences between most groups, except when comparing the 5%

(group II) with the 10% (group III), where no statistically significant difference was observed ( $p = 0.148, p > 0.05$ ) (Table 6).

### DISCUSSION

Dental caries treatments often fail to completely remove all microorganisms, leaving some in residual tissue. Without effective seals, cariogenic bacteria can cause recurrent caries and restoration failure.<sup>16</sup> A solution is to use dental materials with bacteriostatic and bactericidal properties. Enhancing conventional GIC with plant-based nanoparticles can improve both its mechanical and antibacterial properties, addressing the limitations of traditional GIC. Nanoparticles offer medicinal benefits and cost-effectiveness

**Table 4:** Pairwise comparison of strength and microhardness of phyto-mediated nanocomposite (Ch-Ti-Zr-HA)-modified GIC and conventional GIC

Variables	Pairwise comparison	Mean difference	Std. error	95% confidence interval		p-value
				Lower bound	Upper bound	
Compressive	3 vs 5%	-11.175	0.216	-11.754	-10.595	0.001*
	3 vs 10%	-18.716	0.216	-19.296	-18.137	0.001*
	3% vs control	10.716	0.216	10.137	11.296	0.001*
	5 vs 10%	-7.541	0.216	-8.121	-6.962	0.001*
	5% vs control	21.891	0.216	21.312	22.471	0.001*
	10% vs control	29.433	0.216	28.854	30.012	0.001*
Flexural	3 vs 5%	-4.546	0.068	-4.730	-4.362	0.001*
	3 vs 10%	-7.593	0.068	-7.777	-7.409	0.001*
	3% vs control	10.264	0.068	10.080	10.448	0.001*
	5 vs 10%	-3.046	0.068	-3.230	-2.862	0.001*
	5% vs control	14.810	0.068	14.627	14.994	0.001*
	10% vs control	17.857	0.068	17.673	18.041	0.001*
Microhardness	3 vs 5%	-3.132	0.086	-3.362	-2.902	0.001*
	3 vs 10%	-4.90417*	0.086	-5.134	-4.674	0.001*
	3% vs control	3.79750*	0.086	3.567	4.027	0.001*
	5 vs 10%	-1.77167*	0.086	-2.001	-1.541	0.001*
	5% vs control	6.93000*	0.086	6.700	7.159	0.001*
	10% vs control	8.70167*	0.086	8.471	8.931	0.001*

\*p-value was significant at 0.05. The p-value was derived from the multiple comparison Tukey HSD test

**Table 5:** Comparison of solubility of phyto-mediated nanocomposite (Ch-Ti-Zr-HA)-modified GIC and conventional GIC

Groups	N	Mean $\pm$ SD	Std. error	Lower bound	Upper bound	F value	p-value
3%	6	0.086 $\pm$ 0.005	0.0021	0.081	0.092	148.33	0.001*
5%	6	0.056 $\pm$ 0.005	0.0021	0.051	0.062		
10%	6	0.063 $\pm$ 0.005	0.0021	0.057	0.068		
Control	6	0.113 $\pm$ 0.005	0.0021	0.107	0.118		

\*Statistically significant value of  $p < 0.05$ . The p-value was derived from a one-way ANOVA test

**Table 6:** Pairwise comparison of solubility of phyto-mediated nanocomposite (Ch-Ti-Zr-HA)-modified GIC and conventional GIC

Pairwise comparison	Mean difference	Std. error	95% confidence interval		p-value
			Lower bound	Upper bound	
3 vs 5%	0.0300	0.002	0.021	0.038	0.001*
3 vs 10%	0.0233	0.002	0.014	0.031	0.001*
3% vs control	-0.0266	0.002	-0.035	-0.018	0.001*
5 vs 10%	-0.0066	0.002	-0.015	0.001	0.148
5 vs control	-0.0566	0.002	-0.065	-0.048	0.001*
10% vs control	-0.0500	0.002	-0.058	-0.041	0.001*

\*p-value was significant at 0.05. The p-value was derived from the multiple comparison Tukey HSD test

while avoiding antibacterial resistance. Integrating nanomaterials into the GIC matrix can enhance its performance.

Mechanical properties are crucial for dental restorative materials, which must endure the forces from chewing.<sup>17</sup> These materials need to be strong enough to handle the repetitive stress of mastication, which averages 200–400 N.<sup>18</sup> The ability of a material to resist applied forces is influenced by its atomic bonds and material properties. Compressive strength, which measures the maximum stress a material can bear before fracturing, is particularly relevant for brittle materials like GIC.<sup>19</sup> It is commonly used to assess the strength of GICs. Type IX GIC was chosen as the control due to its widespread use and recommendation by WHO for ART.<sup>9</sup>

In this study, a nanocomposite system of Ch-Ti-Zr-HA nanoparticles was developed using phyto-mediated synthesis techniques. SEM analysis revealed that the nanoparticles were uniformly distributed within the GIC matrix. Significant enhancements were noted in the compressive and flexural strength, as well as microhardness, of the Ch-Ti-Zr-HA nanocomposite-modified GIC compared to conventional GIC. This improvement is attributed to the fine, evenly dispersed nanocomposite particles, which help distribute external stress more uniformly and prevent excessive stress concentration, thereby strengthening the GIC. The addition of hydroxyapatite (HA) aids in the formation of polysalt bridges, further enhancing mechanical properties.<sup>20</sup> Titanium dioxide (TiO<sub>2</sub>) was included for its chemical stability, biocompatibility, and nontoxicity.<sup>21</sup> Another study stated that HA, due to its similarity to the chemical and structural features of bone and teeth, is well-suited for enhancing GIC applications.<sup>22</sup> Similarly, zirconium dioxide (ZrO<sub>2</sub>) contributes to higher strength, fracture toughness, and biocompatibility, mitigating brittleness and reinforcing the GIC's mechanical properties.<sup>23</sup>

For GICs to effectively prevent dental caries and provide durable restorations, they must exhibit strong antibacterial properties. Our study demonstrated a significant enhancement in antimicrobial efficacy with nanocomposite-modified GICs. This finding is consistent with Alatawi et al.,<sup>24</sup> who reported improved antimicrobial activity in GICs with nano hydroxyapatite (HA). Similarly, Shinonaga et al.<sup>25</sup> found that GICs with incorporated hydroxyapatite showed better antibacterial effects compared to traditional GICs. Moreover, Zaki et al.<sup>26</sup> noted that the absence of secondary caries failures might be attributed to the cariostatic properties of GICs, which release fluoride over time. Tiwari et al. found that zirconia-infused GIC showed the highest antibacterial activity against *S. mutans* compared to conventional GIC.<sup>27</sup> Similarly, Surabhilakshan et al. suggested that zirconia-enriched GIC could be a promising restorative material with anticariogenic properties.<sup>28</sup> Additionally, Kukreja et al. concluded that zirconia-enhanced GIC exhibited maximum antibacterial activity.<sup>29</sup> Ibrahim et al. concluded that introducing chitosan into the liquid phase of GIC resulted in pronounced antibacterial activity,<sup>30</sup> which is consistent with our study, where Ch, Zr, and HA were added, resulting in heightened antimicrobial activity. This effect is likely due to nanoparticles infiltrating bacterial cells, triggering oxidative stress, which inhibits growth and leads to bacterial cell death.

The data indicate that the nanocomposite Ch-Ti-Zr-HA modified GIC showed significantly higher compressive strength compared to the control ( $p < 0.05$ ). This result aligns with previous findings, such as the 4% GIC-HA, which showed higher compressive strength than Fuji IX.<sup>20</sup> Similarly, 5% nanoZrO<sub>2</sub>-SiO<sub>2</sub>-HA GIC improved compressive strength, flexural strength, and hardness over conventional GIC,<sup>31</sup> which aligns with our findings. Moshaverinia

et al. found that GIC enhanced with nano-HA-fluorapatite exhibited better compressive, tensile, and flexural strength than standard GIC.<sup>32</sup> Other studies have also shown improved stress resistance and mechanical properties in GIC modified with nanoparticles and cellulose nanocomposites.<sup>33,34</sup> Singer et al. observed that GIC incorporating plant extracts showed enhanced flexural strength,<sup>35</sup> supporting our results with plant-based nanoparticles. Showkat et al. found improved compressive strength in GIC modified with titanium and nano-HA, similar to our study. GIC with TiO<sub>2</sub> nanopowder showed the highest flexural strength,<sup>20</sup> and Moheet et al. found enhanced microhardness in GIC with 10% nano-HA silica.<sup>36</sup> Gu et al. demonstrated that 4% HA/ZrO<sub>2</sub>-GIC had the highest Vickers hardness.<sup>23</sup> These improvements are attributed to the nanocomposite Ch-Ti-Zr-HA particles filling voids between glass particles, increasing packing density and reinforcing the GIC. The inclusion of nanostructures in GIC led to a reduction in the presence of air voids and internal microcracks. Moreover, these modified materials demonstrated enhanced ease of handling compared to unmodified cements, resulting in significantly higher mechanical properties.

Arita et al. found that adding 8% hydroxyapatite granules to GIC yielded the highest flexural strength.<sup>37</sup> In our study, the 10% nanocomposite Ch-Ti-Zr-HA modified GIC achieved the highest flexural strength of  $34.71 \pm 0.223$ . All experimental groups with nanocomposite Ch-Ti-Zr-HA had superior flexural strength compared to the control group. This enhancement is likely attributed to the toughening effect of ZrO<sub>2</sub> and the added benefits of HA on polysalt bridge formation in the GIC matrix. HA may enhance acid-base reactions in the setting cement, improving mechanical properties. HA also accelerates early flexural strength development in wet conditions.<sup>25</sup> The increase in flexural strength is likely due to nanoparticles filling voids between HA rods, increasing packing density and reducing crack propagation.<sup>15</sup> Thus, the nanocomposite Ch-Ti-Zr-HA modified GIC showed the highest flexural strength among the groups tested.

Solubility impacts both the mechanical and antibacterial properties of dental materials, affecting their longevity. GIC surfaces erode and dissolve when exposed to various liquids, with maximum water absorption typically occurring within the first week.<sup>38</sup> As the acid-base reaction progresses, GIC absorbs water into its structure, and excess water is removed during drying. Our study observed that as Ch-Ti-Zr-HA nanocomposite concentration increased, GIC solubility decreased. This is likely due to the nanocomposite reducing internal pores and stabilizing the GIC matrix, thus lowering its dissolution rate. However, the study's conditions may not fully replicate clinical environments. Clinical factors, such as moisture contamination and mixing techniques, can affect dental cement performance. Future research should consider acidic conditions, saliva, and wear to better understand material characteristics.

## CONCLUSION

The microstructural characterization of the phyto-mediated nanocomposite Ch-Ti-Zr-HA modified GIC, followed by evaluation, revealed the following. SEM analysis revealed nanoscale particles, with spherical ZrO<sub>2</sub> particles filling gaps between rod-shaped HA crystals, resulting in a smoother surface. The nanoparticles were evenly distributed throughout the samples. FTIR spectra identified functional groups for each element, and EDX analysis showed a uniform distribution of ZrO<sub>2</sub>, Ca, and P, with high-density patterns for ZrO<sub>2</sub> and Ca. The modified GIC demonstrated no cytotoxicity,



exhibited favorable anti-inflammatory responses, and showed effective antimicrobial properties. Incorporating nanoCh-Ti-Zr-HA significantly enhanced the compressive and flexural strengths of conventional GIC. The 10% Ch-Ti-Zr-HA modified GIC showed notable improvements in these strengths, as the nanopowder created a denser, stronger cement. This modification improved hardness, suggesting potential for expanded clinical use, particularly in high-stress areas. The Ch-Ti-Zr-HA modified GIC is thus promising as a new biomaterial with excellent biocompatibility and mechanical properties, suitable for core materials and posterior restorations.

## ORCID

Jessy Paulraj  <https://orcid.org/0000-0001-9231-6077>

## REFERENCES

- Yamakami SA, Ubaldini ALM, Sato F, et al. Study of the chemical interaction between a high-viscosity glass ionomer cement and dentin. *J Appl Oral Sci* 2018;26:e20170384. DOI: 10.1590/1678-7757-2017-0384
- Pavithra AS, Paulraj J, Rajeshkumar S, et al. Comparative evaluation of antimicrobial activity and compressive strength of conventional and thyme-modified glass ionomer cement. *Ann Dent Spec* 2023;11(1):70–77. DOI: 10.51847/FrmCSw6TqP
- Sun L, Yan Z, Duan Y, et al. Improvement of the mechanical, tribological and antibacterial properties of glass ionomer cements by fluorinated graphene. *Dent Mater*. 2018;34(6):e115–e127. DOI: 10.1016/j.dental.2018.02.006
- Paulraj J, Nagar P. Antimicrobial efficacy of triphala and propolis modified glass ionomer cement: an in vitro study. *Int J Clin Pediatr Dent* 2020;13(5):457–462. DOI: 10.5005/jp-journals-10005-1806
- Hebling J, Giro EM, Costa CA. Human pulp response after an adhesive system application in deep cavities. *J Dent* 1999;27:557. DOI: 10.1016/S0300-5712(99)00034-2
- Mahalakshmi S, Chowdhary N, Shivanna V. et al. Comparative evaluation of mechanical properties of conventional glass ionomer cement incorporated with nonfluoridated remineralizing agents. *Int J Clin Pediatr Dent* 2024;17(2):125–129. DOI: 10.5005/jp-journals-10005-2728
- Nishanthine C, Miglani R, Indira R, et al. Evaluation of fluoride release in chitosan-modified glass ionomer cements. *Int Dent J* 2022;72(6):785–791. DOI: 10.1016/j.identj.2022.05.005
- Moheet IA, Luddin N, Ab Rahman I, et al. Novel nano-hydroxyapatite-silica-added glass ionomer cement for dental application: evaluation of surface roughness and sol-sorption. *Polym Polym Compos* 2020;28(5):299–308. DOI: 10.1177/0967391119874678
- Arita K, Yamamoto A, Shinonaga Y, et al. Hydroxyapatite particle characteristics influence the enhancement of the mechanical and chemical properties of conventional restorative glass ionomer cement. *Dent Mater J* 2011;30:672–683.
- Shiekh RA, Ab Rahman I, Luddin N. Modification of glass ionomer cement by incorporating hydroxyapatite-silica nano-powder composite: sol-gel synthesis and characterization. *Ceram Int* 2014;40:3165–3170.
- Rajabzadeh G, Salehi S, Nemati A, et al. Enhancing glass ionomer cement features by using the HA/YSZ nanocomposite: a feed forward neural network modelling. *J Mech Behav Biomed Mater* 2014;29:317–327.
- Silva VV, Lameiras FS, Lobato ZI. Biological reactivity of zirconia-hydroxyapatite composites. *J Biomed Mater Res* 2002;63:583–590.
- Rahman IA, Ghazali NAM, Bakar WZW, et al. Modification of glass ionomer cement by incorporating nanozirconia-hydroxyapatite-silica nano-powder composite by the one-pot technique for hardness and aesthetics improvement. *Ceram Int* 2017;43:13247–13253.
- Rahman IA, Masudi SAM, Luddin N, et al. One-pot synthesis of hydroxyapatite-silica nanopowder composite for hardness enhancement of glass ionomer cement (GIC). *B Mater Sci* 2014;37:213–219.
- Moheet IA, Luddin N, Ab Rahman I, et al. Evaluation of mechanical properties and bond strength of nano-hydroxyapatite-silica added glass ionomer cement. *Ceram Int* 2018;44:9899–9906.
- Marit SS, Anita A, Wendt KL, et al. Dental caries in children and adolescents. In: Koch G, Poulsen S, Espelid I, Dorte H, editors. *Pediatric Dentistry: A Clinical Approach*. 3rd ed. Hoboken: John Wiley & Sons; 2016. p. 102.
- Sharmila R, Maiti S, Jessy P. Comparative analysis of abrasion resistance in relation to different temporary acrylic crown material using tooth brush simulator-an in vitro study. *Int J Dentistry Oral Sci* 2021;8(4):2153–2157. DOI: 10.19070/2377-8075-21000425
- Takaki P, Vieira M, Bommarito S. Maximum bite force analysis in different age groups. *Int Arch Otorhinolaryngol* 2014;18:272–276.
- Mount GJ. Some physical and biological properties of glass ionomer cement. *Int Dent J* 1995;45:135–140.
- Showkat I, Chaudhary S, Sinha AA, et al. Comparative evaluation of flexural strength of conventional glass ionomer cement and glass ionomer cement modified with chitosan, titanium dioxide nanopowder and nanohydroxyapatite: an in vitro study. *Int J Clin Pediatr Dent* 2023;16:S72–S76. DOI: 10.5005/jp-journals-10005-2617
- Elsaka SE, Hamouda IM, Swain MV. Titanium dioxide nanoparticles addition to a conventional glassionomer restorative: influence on physical and antibacterial properties. *J Dent* 2011;39:589–598. DOI: 10.1016/j.jdent.2011.05.006
- Ilancheran P, Paulraj J, Maiti S, et al. Green synthesis, characterization, and evaluation of the antimicrobial properties and compressive strength of hydroxyapatite nanoparticle-incorporated glass ionomer cement. *Cureus* 2024;16(4):e58562. DOI: 10.7759/cureus.58562
- Gu YW, Yap AU, Cheang P, et al. Effects of incorporation of HA/ZrO<sub>2</sub> into glass ionomer cement (GIC). *Biomaterials* 2005;26:713–720.
- Alatawi RAS, Elsayed NH, Mohamed WS. Influence of hydroxyapatite nanoparticles on the properties of glass ionomer cement. *J Mater Res Technol* 2019;8:344–349. DOI: 10.1016/j.jmrt.2018.01.010
- Shinonaga Y, Arita K, Nishimura T, et al. Effects of porous-hydroxyapatite incorporated into glass-ionomer sealants. *Dent Mater J* 2015;34:196–202. DOI: 10.4012/dmj.2014-195
- Zaki ZM, Niazzy MA, Zaazou MH, et al. Effect of incorporation of nano-hydroxyapatite particles on the clinical performance of conventional and resin-modified glass ionomer cement in class V cavities: split-mouth, randomized controlled trial. *Bull Natl Res Cent* 2021;45:199. DOI: 10.1186/s42269-021-00655-2
- Tiwari S, Kenchappa M, Bhayya D, et al. Antibacterial activity and fluoride release of glass-ionomer cement, compomer and zirconia reinforced glass-ionomer cement. *J Clin Diagn Res* 2016;10:90–93. DOI: 10.7860/JCDR/2016/16282.7676
- Surabhilakshan SL, Gopinath AS, Joseph S, et al. Comparative evaluation of fluoride release and recharge of zirconia-reinforced, resin-modified, and conventional glass ionomer cements. *World J Dent* 2021;12:469–473. DOI: 10.5005/jp-journals-10015-1877
- Kukreja R, Singla S, Bhadoria N, et al. An in vitro study to compare the release of fluoride from glass ionomer cement (Fuji IX) and zirconomer. *Int J Clin Pediatr Dent* 2022;15:35–37. DOI: 10.5005/jp-journals-10005-2141
- Ibrahim MA, Meera Priyadarshini B, Neo J, et al. Characterization of chitosan/TiO<sub>2</sub> nano-powder modified glass-ionomer cement for restorative dental applications. *J Esthet Restor Dent* 2017;29(2):146–156. DOI: 10.1111/jerd.12282
- Sajjad A, Bakar WZW, Mohamad D, et al. Characterization and enhancement of physico-mechanical properties of glass ionomer cement by incorporating a novel nano zirconia silica hydroxyapatite composite synthesized via sol-gel. *AIMS Mater Sci* 2019;6(5):730–747. DOI: 10.3934/mat.2019.5.730
- Moshaverinia A, Ansari S, Moshaverinia M, et al. Effects of incorporation of hydroxyapatite and fluoroapatite nanobioceramics

- into conventional glass ionomer cements (GIC). *Acta Biomater* 2008;4:432–440. DOI: 10.1016/j.actbio.2007.07.011
33. Hussainy SN, Nasim I, Thomas T, et al. Clinical performance of resin-modified glass ionomer cement, flowable composite, and polyacid-modified resin composite in noncarious cervical lesions: one-year follow-up. *J Conserv Dent* 2018;21:510. DOI: 10.4103/JCD.JCD\_51\_1835
  34. Saini R, Vaddamanu SK, Kanji MA, et al. Comparison of the antibacterial properties of Resin cements with and without the addition of nanoparticles: a systematic review. *BMC Oral Health* 2024;24(1):1426. DOI: 10.1186/s12903-024-05013-y
  35. Singer L, Bierbaum G, Kehl K, et al. Evaluation of the flexural strength, watersorption, and solubility of a glass ionomer dental cement modified using phytomedicine. *Materials (Basel)* 2020;13(23):5352. DOI: 10.3390/ma13235352
  36. Moheet IA, Luddin N, Rahman IA, et al. Modifications of glass ionomer cement powder by addition of recently fabricated nano-fillers and their effect on the properties: a review. *Eur J Dent* 2019;13:470–477. DOI: 10.1055/s-0039-1693524
  37. Arita K, Lucas ME, Nishino M. The effect of adding hydroxyapatite on the flexural strength of glass ionomer cement. *Dent Mater J* 2003;22:126–136.
  38. Brito CR, Velasco LG, Bonini GA, et al. Glass ionomer cement hardness after different materials for surface protection. *J Biomed Mater Res A* 2010;93(1):243–246. DOI: 10.1002/jbm.a.32524